RESEARCH ARTICLE

Mass spectrometry-based quantification of myocardial protein adducts with acrolein in an in vivo model of oxidative stress

Jianyong Wu[1], *Jan F. Stevens*[2] *and Claudia S. Maier*[1]

[1] Department of Chemistry, Oregon State University, Corvallis OR, USA
[2] Department of Pharmaceutical Sciences and Linus Pauling Institute, Oregon State University, Corvallis OR, USA

Received: April 13, 2011
Revised: June 20, 2011
Accepted: June 29, 2011

Acrolein (ACR) exposure leads to the formation of protein–ACR adducts. Protein modification by ACR has been associated with various chronic diseases including cardiovascular and neurodegenerative diseases. Here, we report an analytical strategy that enables the quantification of Michael-type protein adducts of ACR in mitochondrial proteome samples using liquid chromatography in combination with tandem mass spectrometry and selected ion monitoring (LC-MS/MS SRM) analysis. Our approach combines site-specific identification and relative quantification at the peptide level of protein–ACR adducts in relation to the unmodified protein thiol pool. Treatment of 3-month-old rats with CCl_4, an established in vivo model of acute oxidative stress, resulted in significant increases in the ratios of distinct ACR-adducted peptides to the corresponding unmodified thiol-peptides obtained from proteins that were isolated from cardiac mitochondria. The mitochondrial proteins that were found adducted by ACR were malate dehydrogenase, NADH dehydrogenase [ubiquinone] flavoprotein 1, cytochrome *c* oxidase subunit VIb isoform 1, ATP synthase d chain, and ADP/ATP translocase 1. The findings indicate that protein modification by ACR has potential value as an index of mitochondrial oxidative stress.

Keywords:
Acrolein / Aldehyde/keto-reactive probe / Mitochondria / Protein carbonyls / Selected reaction monitoring

1 Introduction

Humans are exposed to acrolein (ACR) ($CH_2 = CH\text{-}CHO$) from endogenous sources, such as oxidative degradation of polyunsaturated fatty acids, polyamines and threonine, as well as exogenous sources such as heated cooking oil, heat-processed foods containing carbohydrates and amino acids, cigarette smoke, automobile exhaust and industrial emissions [1, 2]. ACR exposure may result in the modification of biological nucleophiles, such as nucleic acids, proteins and peptides [3–5]. Protein adducts of ACR have been associated with various pathophysiological conditions including different types of cancer, diabetes, atherosclerosis, ischemia/reperfusion injury, spinal cord injury and neurodegenerative diseases [6–12]. Michael-type adduction by ACR contributes to protein carbonyl content. Protein carbonylation occurs via diverse chemical pathways, such as backbone peptide bond cleavage and metal-catalyzed side-chain oxidations and Michael-type adduction with 2-enals that include ACR and (other) lipid peroxidation products [13, 14]. Protein carbonyls have also been extensively studied in meat products and other food proteins [15].

Traditionally, protein carbonyls are detected by colorimetric assays using 2,4-dinitrophenylhydrazine (DNPH) [16] or by immunochemical assays using anti-dinitrophenyl antibodies [17, 18]. However, these methods only report on the overall content of protein carbonyls and fail to assign modifications of

Correspondence: Professor Claudia S. Maier, Department of Chemistry, Oregon State University, Corvallis OR, 97330, USA
E-mail: Claudia.maier@oregonstate.edu
Fax: +1-541-737-2062

Abbreviations: ACR, acrolein; **ARP,** aldehyde reactive probe; **HNE,** 4-hydroxy-2-nonenal; **IPB,** iodoacetyl-PEO_2-biotin; **SCX,** strong cation exchange; **SRM,** selected reaction monitoring; **SSM,** subsarcolemmal mitochondria

distinct proteins. Protein carbonyl-specific antibodies have become available, e.g. antibodies against ACR–protein adducts (i.e. N^{ε}-(3-formyl-3,4-dehydropiperidino) (FDP)-lysine [19]) and 4-hydroxy-2-nonenal (HNE)–protein adducts, which allow the detection of protein targets using gel-based approaches. However, site-specific assignments of oxidative modifications are usually not achievable with gel-based approaches. MS-based approaches have emerged that identify sites of oxidative protein modifications in in vitro studies [20–23]. Several groups have reported the use of tandem mass spectrometric approaches for the site-specific identification of protein modifications by 2-enals and other oxidative modifications in cell culture studies, tissues and biofluids [24–30]. Only a few studies have become available that attempt the targeted quantification of protein oxidative modifications using tandem mass spectrometry-based approaches [31, 32]. There is a need for analytical strategies that allow quantification of specific aldehydic protein adducts in relation to the unmodified protein pool in biological systems. Here, we describe a targeted proteomic approach for protein carbonyls in conjunction with a selective MS-based method for the simultaneous detection and quantification of distinct protein–ACR adducts. The MS platform used in this study consisted of a nanoflow liquid chromatography coupled to an electrospray triple quadrupole/linear ion trap mass spectrometer that was operated in the selected reaction monitoring mode (nanoLC-ESI-SRM analysis). This strategy was applied to quantify protein–ACR adducts in cardiac mitochondria in an in vivo rodent model of oxidative stress (Fig. 1).

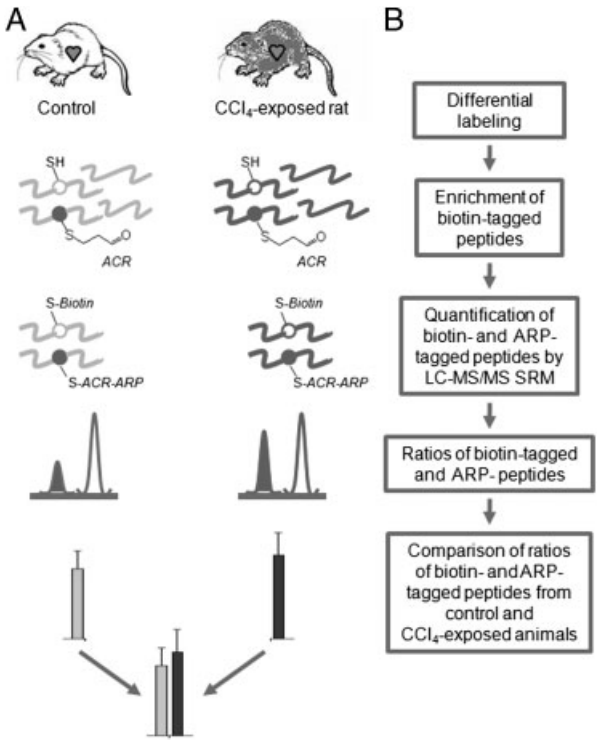

Figure 1. MS-based quantification of distinct protein–acrolein adducts in complex biological mixtures. (A) Schematic presentation of the analytical strategy for determining relative ratios of a distinct protein–ACR adduct to its unmodified protein thiol site using differential labeling chemistry in combination with LC-MS/MS SRM analysis. Protein–ACR adducts are chemoselectively labeled with an aldehyde/keto-specific hydroxylamine-containing biotinylation probe (aka ARP) and thiols are selectively labeled with the thiol-specific biotinylation reagents, iodoacetyl-PEG_2-biotin (IPB). LC-MS/MS SRM analysis is used for obtaining SRM chromatogram of distinct peptide ions. (B) Workflow developed and employed for the assessment of the relative ratio of a distinct protein–ACR adduct to the respective unmodified protein thiol site.

2 Materials and methods

2.1 Chemicals and materials

Sequencing grade-modified trypsin was purchased from Promega (Madison, WI, USA). ACR (≥99%) was obtained from Fluka (St. Louis, MO, USA). Aldehyde-reactive probe (ARP, *N*-aminooxymethylcarbonylhydrazino D-biotin) was purchased from Dojindo Laboratories (Kumamoto, Japan). UltraLink-immobilized monomeric avidin, iodoacetyl-PEG_2-Biotin (IPB) and Triton X-100 detergent were obtained from Pierce (Rockford, IL, USA). Bovine serum albumin (BSA) was from Calbiochem (LA, CA, USA). Macrospin strong cation exchange (SCX) columns were from Nest Group (Southborough, MA, USA).

2.2 Animal treatment

The experimental protocol for the animal studies was approved by the Institutional Animal Care and Use Committee at Oregon State University (ACUP 3770). Seven Male F344 rats (Harlan, Indianapolis, IN, USA) were housed individually in plastic cages covered with Hepa filters. The animals were allowed free access to standard animal chow and water ad libitum. After 1 wk of acclimatization, one 25-month-old rat was sacrificed for an analytical reproducibility study and the other six 3-month-old rats were transferred to metabolism cages. These six animals were divided into two groups of three, with one group receiving an intraperitoneal dose of 1 mL/kg CCl_4 (dissolved in corn oil) and the other group (control) receiving the vehicle alone. The CCl_4 dose of 1 mL/kg was chosen on the basis of literature reports [33, 34]. The rats were sacrificed 24 h after the treatment.

2.3 Preparation of IPB-labeled and ARP-ACR-modified BSA peptides

A solution of BSA (2 mg) in 1.0 mL of phosphate buffer (20 mM, pH 8.2) was reacted with 25 μL of DTT (60 mM in

20 mM phosphate buffer, pH 8.3) at 95°C for 10 min. One half of the reduced BSA solution was then mixed with 200 μL 20 mM IPB in 50 mM phosphate buffer, (pH 8.3). The mixture was kept in dark at room temperature for 90 min to form IPB-labeled BSA. Excess reagent was removed by adding 30 μL DTT (60 mM in 20 mM phosphate buffer, pH 8.3). The other half of the reduced BSA was reacted with 60 μL of ACR (80 mM in 20 mM phosphate buffer, pH 8.3) at room temperature for 60 min. The excess of ACR was removed by adding 40 μL DTT (60 mM in 20 mM phosphate buffer, pH 8.3). The ACR-modified BSA was then reacted with 250 μL ARP (30 mM in H_2O) at room temperature for 60 min. Both ARP-ACR-modified and IPB-labeled BSA were digested with trypsin and passed through an ultrafiltration membrane (10 kDa MWCO). The peptide encompassing the residues 286 and 297 of BSA, YIC*DNQDTISSK modified on the cysteine residue (marked with an asterisk) with the ARP-ACR and IPB moiety, respectively, was used for method development.

2.4 Mitochondrial preparations

Mitochondria were isolated from rat hearts and separated by differential centrifugation to obtain subsarcolemmal mitochondria (SSM) [35]. Mitochondria were stored at −80°C. Each sample of SSM containing approximately 0.5 mg total protein was washed twice with phosphate buffer (10 mM NaH_2PO_4 pH 7.4) at 0°C. The mitochondria were then resuspended in 400 μL of 10 mM NaH_2PO_4 (pH 7.4) containing 1% Trition X-100 detergent and 3 mM DTT. DTT was added to prevent thiol modifications by reactive species during sample preparation. The mitochondria were sonicated in ice water for 5 min to solubilize the proteins. The soluble protein fraction was obtained by centrifugation at 14 000 × *g* for 15 min at 4°C. The supernatant was then filtered through an Amicon Microcon centrifugal filter (10 kDa MWCO) to remove low-molecular-weight molecules at 4°C. Mitochondrial proteins were re-suspended in 400 μL of 10 mM NaH_2PO_4 (pH 7.4) containing 1 mM DTT. Further sample preparation was as follows (Supporting Information Fig. S19).

(i) Proteins were labeled with ARP for 1 h at room temperature. The final ARP concentration was 3 mM. Proteins were digested with a 1:50 ratio of trypsin at 37°C for 15 h.

(ii) 15 μL DTT (30 mM in 20 mM phosphate buffer, pH 8.0) was added to the tryptic peptides to reduce disulfide bonds. The sample was then filtered through an Amicon Microcon centrifugal filter (10 kDa MWCO) to remove trypsin.

(iii) 40 μL of the sample was added to 120 μL IPB (5 mM, 50 mM Tris buffer, pH 8.3). The alkylation reaction was performed in dark at room temperature for 90 min to form IPB-labeled peptides. Unreacted IPB was trapped with 80 μL DTT (30 mM in 20 mM phosphate buffer, pH 8.0). The reaction mixture was diluted with water to a volume of 1750 μL.

(iv) 35 μL of the sample from step 3 (IPB-modified peptides) were mixed with 800 μL of the sample from step 2 (ARP-labeled peptides). The mixed sample was then subjected to SCX and affinity chromatography, and stored at −20°C prior to LC-MS/MS SRM analysis.

2.5 SCX cleanup

Modified peptides were purified by SCX chromatography using Macrospin SCX columns (Nest Group, Southborough, MA, USA). ACN was used to activate the column. An elution buffer consisting of 20% ACN in 10 mM potassium phosphate buffer/0.6 M KCl (adjusted to pH 3 with H_3PO_4) was applied to condition the column. A washing buffer (10 mM potassium phosphate, 10 mM KCl, pH 3.0) containing 20% ACN was used to equilibrate the column. Peptide samples (~pH 3.0, adjusted with H_3PO_4) were applied to the conditioned column and rinsed with washing buffer three times to remove Triton X-100 detergent and unbound components. Finally, 350 μL elution buffer was applied for the columns to release the peptides.

2.6 Affinity chromatography

Ultralink monomeric avidin (200 μL, Pierce, Rockford, IL, USA) was packed into Handee Mini Spin Columns (Pierce Rockford, IL, USA) following the manufacturer's protocol. Columns were washed with 1.5 mL of 10 mM NaH_2PO_4, pH 7.4. Irreversible binding sites, consisting of tetrameric avidin, were blocked by washing with 600 μL of 2 mM D-biotin. To remove excess D-biotin, columns were washed with 1 mL of 2 M glycine-HCl (pH 2.8). The columns were then re-equilibrated by washing twice with 2 mL of phosphate-buffered saline (PBS, 20 mM NaH_2PO_4, 300 mM NaCl). The peptide samples were then slowly added to the affinity columns. To remove non-labeled and non-specifically bound peptides the column was washed twice with 1 mL PBS followed by 1 mL of 10 mM NaH_2PO_4 (pH 7.4) and finally 1.5 mL of 50 mM NH_4HCO_3 containing 20% CH_3OH. The columns were then rinsed with 1 mL of MilliQ H_2O before eluting the ARP-labeled peptides with 0.4% aqueous formic acid containing 20% ACN. Collected fractions were concentrated using a freeze dryer and stored at −20°C prior to MS analysis.

2.7 Nano-HPLC

An Ultimate LC Packing system (Dionex, Sunnyvale, CA, USA) was used. Peptide samples were loaded onto a 5 mm × 0.50 mm C18 trap cartridge (Dionex) at a flow rate of 20 μL/min. After 4 min the trap cartridge was auto-

matically switched in-line to a 75 μm i.d. × 15 cm C18 PepMap 100 column (Dionex). Peptides were eluted using a gradient from 9 to 18% solvent B in A over 90 min at 0.260 μL/min. Solvent A was 1% aqueous ACN containing 0.1% formic acid and solvent B was ACN containing 0.1% formic acid.

2.8 MS

All LC-MS/MS analyses were carried out on a 4000 Q-Trap hybrid tandem mass spectrometer (AB/MDS SCIEX, Concord, ON, Canada) equipped with a nano-ESI source. The electrospray voltage was set to 2300 V and the declustering potential was 60 V. For the identification of ARP-labeled peptides, precursor ion scanning was performed over a mass range of 400–1300 amu at 500 amu/s (Q1 and Q3 with unit resolution).

An enhanced product ion scan (MS/MS) was performed if the intensity of any of the precursors of *m/z* 227 exceeded the threshold value of 1000 counts/s (cps). The scan rate for MS/MS was set to 4000 amu/s. Tandem mass spectral data were analyzed using MASCOT v2.1 (Matrix Science, London, UK) as described previously [21, 36]. The Swiss Prot database v50 (270778 sequences, 99412397 residues) was searched using the following parameters: taxonomy rodentia (20991 sequences), ±0.5 Da mass tolerances for the precursor and fragment ions, possibility of 2 missed proteolytic cleavage sites, with trypsin/P or semitrypsin selected as the digesting enzyme, and ARP-ACR (CHK), ARP-HNE (CHK), ARP-ONE (CHK), ARP-HHE (CHK), ARP-MDA (KR), ARP-β-hydroxyacrolein, ARP-crotonaldehyde selected as variable modifications at the residues specified in parenthesis. Fragment ion assignments were verified and probe-specific ions were annotated manually.

The SRM analyses were conducted with Q1 and Q3 sets at unit resolution. Each SRM transition period was 30 ms. SRM collision energies were 50 and 51 eV for ARP–ACR-modified and IPB-labeled model peptides. For the mitochondrial peptides the collision energies used for the SRM analyses are listed in Table 1.

MALDI MS was performed with an ABI 4700 Proteomics Analyzer with TOF/TOF optics and equipped with a 200-Hz frequency-tripled Nd:YAG laser operating at a wavelength of 355 nm (Applied Biosystems, Framingham, MA, USA). Mass spectra were obtained over a range of *m/z* 700–4000 in the reflectron mode. External mass calibration was applied using the ABI 4700 calibration mixture consisting of the following peptides des-Arg^1-bradykinin ($[M+H]^+$, m/z_{calc} 904.4675), angiotensin I ($[M+H]^+$, m/z_{calc} 1296.6847), Glu^1-fibrinopeptide B ($[M+H]^+$, m/z_{calc} 1570.6768), and ACTH 18-39 ($[M+H]^+$, m/z_{calc} 2465.1983). Peptide samples were cleaned up prior to MS analyses with C18 ZipTips (Millipore, Billerica, MA, USA) following the manufacture's protocol. Peptides were mixed with α-cyano-4-hydroxycinnamic acid (2 mg/mL in 50% ACN containing 0.1% TFA) and 0.5 μL of the mixture was spotted onto a 144-spot stainless steel target plate.

Table 1. SRM parameters and retention times for ARP-ACR (*) and IPB (#) labeled peptides

Peptide[a)]	SRM transition Precursor *m/z* (charge state) → Fragment ion *m/z* (charge state)	Collision energy (eV)	Retention time (min)
a*	783.5 (2+) → 1005.5 (y_6^*, 1+)	40	63.5
a#	805.8 (2+) → 1050.5 ($y_6^\#$, 1+)	41	65
b*	978.9 (2+) → 1205.6 (y_7^*, 1+)	49	75
b#	1001.4 (2+) → 1250.6 ($y_7^\#$, 1+)	50	76.5
c*	825.8 (2+) → 619.3 (y_6, 1+)	42	42.5
c#	848.4 (2+) → 619.3 (y_6, 1+)	43	45
d*	820.3 (2+) → 1125.5 (y_5^*, 1+)	42	64.5
d#	842.8 (2+) → 1170.5 ($y_5^\#$, 1+)	43	66
e*	686.3 (2+) → 289.2 (y_3, 1+)	36	50
e#	708.9 (2+) → 289.2 (y_3, 1+)	37	54
f*	825.9 (2+) → 596.3 (y_6, 1+)	42	67
f#	848.5 (2+) → 596.3 (y_6, 1+)	43	68.5
g*	842.0 (2+) → 678.3 (y_9^*, 2+)	43	72
g#	864.5 (2+) → 700.9 ($y_9^\#$, 2+)	44	72

a) For peptide assignment, sequence information, biological function see Table 2.

3 Results and discussion

3.1 Analytical strategy to quantify distinct protein–ACR adducts in proteomes

We have recently completed a qualitative profiling study of protein adducts of lipoxidation products in the SSM from hearts of 24-month-old rats [36]. This study identified a diverse set of protein lipoxidation adducts. The majority of the assigned adducts were Michael-type ACR adducts with cysteine residues [36]. Here, we report a strategy that enables the quantification of distinct cysteine–ACR adducts at the peptide level which is based on differential chemical tagging of the ACR adducts and the corresponding thiol-containing peptides (Fig. 1). In order to determine the ratios of ACR-modified peptides to their corresponding, i.e. unmodified, thiol-peptides in biological matrices we used *N'*-amino-oxymethylcarbonyl-hydrazino-D-biotin as an aldehyde/keto reactive probe (ARP) as described by us previously [21] and IPB as a chemoselective tagging reagent for thiol-peptides (Fig. 2). The combined use of ARP and IPB allowed biotin-based enrichment and analysis by nano-LC MS/MS using SRM of both analyte groups concomitantly. The use of SRM MS enabled the targeted relative quantification of both analyte groups, i.e. ARP-labeled cysteine–ACR adducts and the corresponding IPB-labeled thiols, at the peptide level with high specificity and sensitivity (Fig. 1).

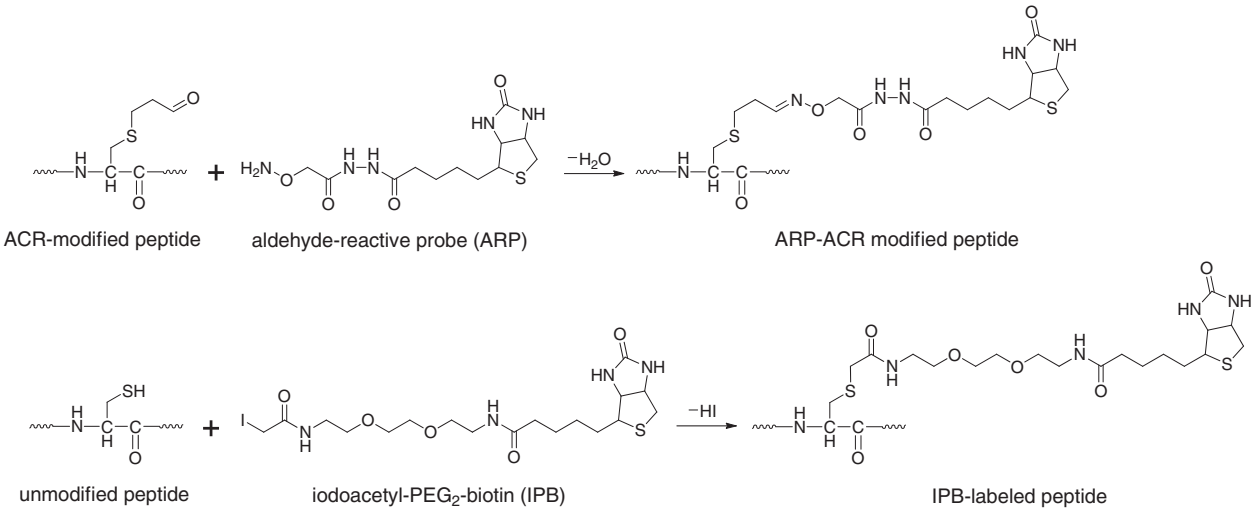

Figure 2. Structures and formations of ARP-ACR-modified and IPB-labeled peptides.

3.2 Development and assessment of a MS-based strategy for the quantification of peptide–ACR adducts

We first tested the reaction yields for the two labeling reactions using a small, commercially available cysteine-containing model peptide, CLLLSAPRR (MH^+, *m/z* 1028.6). The model peptide was reacted with ACR to yield an ACR-modified peptide, which was further reacted with ARP to form an ARP-ACR modified peptide (MH^+, *m/z* 1397.8). The model peptide was also reacted with IPB to form an IPB-labeled peptide (MH^+, *m/z* 1442.8). The MALDI MS spectra of the two crude products indicated that the thiol and ACR-modified peptide were converted into the IPB and ARP derivatives, respectively (Supporting Information Fig. S1).

We next tested our analytical strategy using a tryptic digest of BSA containing ARP-ACR modified and IPB-labeled peptides. For this purpose, BSA was reduced with DTT and the reduced BSA solution was divided into two aliquots. One aliquot was treated with IPB, while the other aliquot was treated with ACR and reacted with ARP. Both modified BSA samples were then digested with trypsin. The peptide YICDNQDTISSK, residues 286–297 of BSA with ARP-ACR and IPB modification, respectively, was used for the proof-of-concept experiment. The other tryptic peptides were considered as background matrix. The nanoLC-ESI-MS/MS spectra of the IPB-labeled peptide and the ARP-ACR-modified peptides are depicted in Figs. S2 and S3. Three fragment ions (y_3, y_5, and y_6) were selected for nanoLC-ESI-MS/MS SRM analysis. Figure S4 shows the SRM chromatograms for 100 fmol of ARP-labeled peptide ACR adduct and 100 fmol IPB-labeled peptide. The SRM peak areas of the ARP-ACR-modified peptide were equivalent to those obtained for the IPB-labeled peptide, implying that the two differently modified peptides had comparable ionization and fragmentation characteristics.

To test the suitability of our strategy for quantification, three SRM standard curves were constructed using 100 fmol IPB-labeled BSA peptide (aa 286–297) as a reference. The amount of ARP-ACR-modified peptide (analyte) was varied between 10.0 and 1000 fmol (Fig. S5). LC-SRM experiments were conducted by monitoring three transitions for the analyte peptide and the corresponding transitions for the reference peptide. The following transitions were monitored for the ARP-ACR-modified peptide (analyte): *m/z* 878.4 (MH_2^{2+}) → *m/z* 321.2 (y_3), *m/z* 878.4 (MH_2^{2+}) → *m/z* 535.3 (y_5) and *m/z* 878.4 (MH_2^{2+}) → *m/z* 650.3 (y_6). For the corresponding IPB-labeled peptide the following SRM transitions were used: *m/z* 900.9 (MH_2^{2+}) → *m/z* 321.3 (y_3), *m/z* 900.9 (MH_2^{2+}) → *m/z* 535.3 (y_5), and *m/z* 900.9 (MH_2^{2+}) → *m/z* 650.3 (y_6). From the SRM chromatograms the peak area for each transition pair were extracted and the peak area ratios determined. To construct the standard curves for each of the three transition pairs monitored the peak area ratio (analyte-to-reference) were plotted as a function of amount ratio (analyte-to-reference). Linear regression analysis yielded slopes of 0.979, 1.102 and 1.100 for each transition pair monitored (Fig. S5). The R^2 was higher than 0.997. For the subsequent mitochondrial proteome analyses, we therefore assumed for the transition pairs monitored a response factor of 1. Thus, the amount ratio between ARP-ACR and IPB-labeled peptides was directly derivable from the ratio of the peak areas extracted from the SRM chromatograms.

3.3 Site-specific identification of mitochondrial protein–ACR adducts

In our previous work, profiling of oxidative modification sites was based on tandem mass spectrometry of ARP-tagged aldehydic protein adducts [29, 37]. Tandem mass spectra of ARP-labeled protein lipoxidation adducts showed a fragment

ion at *m/z* 227.1 which originates from the ARP moiety (F_1, Fig. S18A) [37]. Thus, we used this probe-specific feature to identify protein adducts of lipoxidation products in the current mitochondrial preparations. We conducted precursor ion scanning experiments to trigger the acquisition of full-scan tandem mass spectra for identifying the targets of lipoxidation. This assay consistently yielded seven ACR-modified peptides with ACR modifications on distinct cysteine residues of five mitochondrial proteins. The ACR-modified Cys-containing peptides are listed in Table 2 and are labeled as **a–g**. The modified sites were also found as targets of ACR adduction in our previously described study [36]. The modified proteins are involved in mitochondrial energy production (TCA cycle and oxidative phosphorylation) and ADP/ATP transport (Table 2) [38, 39]. The peptide adducts **a–g** were subsequently selected for quantification using LC-MS/MS SRM analysis.

3.4 CID-based fragmentation of ARP-labeled peptide–ACR adducts and IPB-labeled peptides

In order to use these distinct modification sites for quantification we first conducted a series of tandem mass spectral experiments to obtain optimized CID parameters for the ARP-labeled peptide–ACR adducts and the IPB-alkylated thiol peptides. The tandem spectrum for the EFNGLGDCLTK peptide derived from ADP/ATP translocase 1 is shown in Fig. 3. The fragmentation spectrum of the doubly charged ion of the ARP-labeled peptide–ACR adduct (MH_2^{2+}, *m/z* 783.5) showed mainly y_n and b_n-type ions, which are typically observed in ESI-MS/MS studies with low-energy CID conditions. Similarly, the tandem mass spectrum of the IPB-labeled EFNGLGDCLTK peptide (MH_2^{2+}, *m/z* 805.8) showed the corresponding y_n and b_n-type ions. Examination of the mass spectral data indicated that the fragmentation pattern of the peptide modified by ARP-ACR (+369.2 Da) moiety was analogous to the fragmentation pattern of the corresponding peptide alkylated with IPB (+414.2 Da). The relative fragment ion intensity of the y_n or b_n-type ions was also comparable for the ARP-ACR and IPB-labeled peptide. Both fragment ion spectra showed probe-specific ions. The ARP-ACR-labeled peptide yielded two characteristic ions, F_1 (*m/z* 227.1) and F_2 (*m/z* 332.1) (Fig. 3A and Fig. S18A). Whereas in the spectra of the IPB-labeled peptide the IPB-specific fragment ions, F_a (*m/z* 270.1) and F_b (*m/z* 332.2) were observed (Fig. 3B and Fig. S18B). The tandem mass spectra for the other ARP-labeled peptide–ACR adducts and the respective IPB-labeled peptides are provided in the Supporting Information (Figs. S6–S17).

3.5 Quantification of protein–ACR adducts in cardiac mitochondria

Because the fraction of a distinct ACR adduct in the endogenous protein thiol pool is very low, an analytical workflow was needed that enabled the quantification of ACR-modified peptides and the respective peptide thiols in one LC-MS/MS SRM-run. Figure S19 outlines the adopted workflow to circumvent the substantial concentration difference between ACR-modified peptides and their corresponding peptide thiols, and to avoid problems with the dynamic range of the mass spectrometer and overloading of the nanoLC column. Accordingly, 800 μL of ARP-labeled ACR-peptide digest was used, but only 35 μL of IPB-modified digest was used. Thus, only a fraction of the IPB-modified digest (0.8 μL; derived from 40 μL × 35 μL/1750 μL = 0.8 μL) was ultimately used for nanoLC SRM analysis. Consequently, to calculate the ratio of the ARP-ACR-modified peptides to the IPB-labeled peptides in the original mitochondrial samples the peak area ratios of ARP-ACR-modified peptide to IPB-labeled peptides obtained from nanoLC-SRM analysis in the combined sample were divided by 1000 (derived from 800 μL/0.8 μL).

For the quantitative analyses, for each peptide three SRM transitions were constructed based on fragment ions that were observed for the ARP-labeled peptide–ACR adduct as well as for the respective IPB-labeled thiol peptide. In Fig. 3 and Figs. S6–S17 the fragment ions that were used for the SRM transitions are encircled. For each LC-MS/MS SRM analysis 42 transitions were monitored. Representative SRM chromatograms for the seven ARP-ACR-modified peptides and their corresponding IPB-labeled peptides are shown in

Table 2. Summary of the acrolein-modified peptides (labeled **a–g**) quantified in this study

Peptide	Modified residue	Protein name	Biological function
a. EFNGLGD**C**LTK	**C**159	ADP/ATP translocase 1	Transport
b. GADIMYTGTVD**C**WR	**C**256		
c. N**C**AQFVTGSQAR	**C**100	ATP synthase d chain	Respiratory chain (complex V)
d. GGDVSV**C**EWYR	**C**54	Cytochrome c oxidase subunit VIb isoform 1	Respiratory chain (complex IV)
e. LVEG**C**LVGGR	**C**142	NADH dehydrogenase [ubiquinone] flavoprotein 1	Respiratory chain (complex I)
f. G**C**DVVVIPAGVPR	**C**93	Malate dehydrogenase	TCA cycle
g. TIIPLISQ**C**TPK	**C**212		

Peptide sequences, biological and functional assignments were made on the basis of information from the NCBI (http://www.ncbi.nlm.nih.gov/Pubmed) and the UniPort Knowledgebase (http://www.uniprot.org) websites.

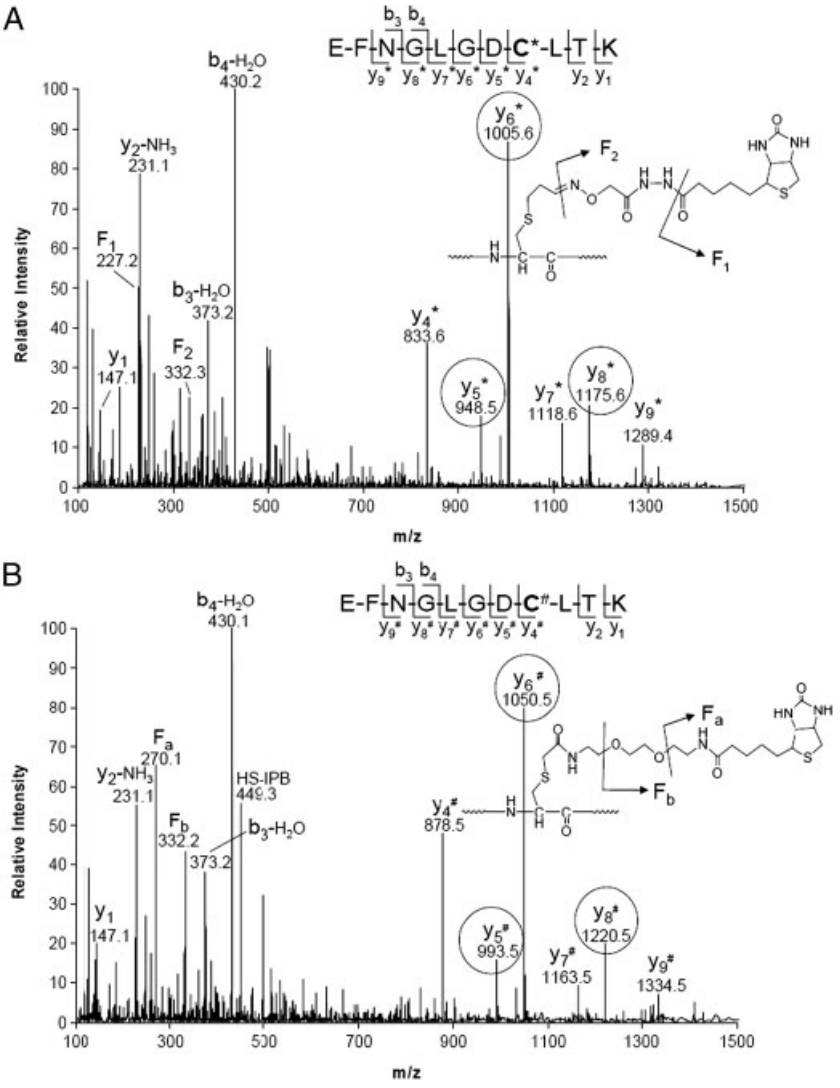

Figure 3. Tandem mass spectra of the doubly charged peptide a with different modifications from ADP/ATP translocase 1 by ESI low-energy CID: (A), ARP-ACR modified (MH_2^{2+}, *m/z* 783.5); (B) IPB labeled (MH_2^{2+}, *m/z* 805.8). The encircled fragments were used for SRM analysis.

Fig. S20. The ARP-ACR-modified peptides usually eluted at shorter retention times than the corresponding IPB-labeled peptides. The chromatographic peak widths of the ARP-ACR-modified peptides were usually larger than the peak widths observed for the corresponding IPB-labeled peptides. To compensate for the mass difference of 45 Da between ARP-ACR and IPB-labeled peptides, the collision energy for the IPB-labeled peptide ions was set 1 eV higher than the collision energy used for the corresponding ARP-ACR-modified peptide ions. Detailed information on the SRM parameters used for the quantitative analysis of the APR-ACR and IPB-labeled peptides are given in Table 1.

We also evaluated the precision of our method. Three mitochondrial preparations from one 25-month-old rat were carried through sample derivatization, enrichment and nanoLC SRM analysis. The results are shown in Table S1. The coefficient of variation (CV) for these three samples was around 5%. The ratio of ACR-modified peptide to the corresponding thiol peptide was found to vary from 4×10^{-4} to 1×10^{-3}. Noteworthy, for ADP/ATP translocase 1 and malate dehydrogenase two distinct adduction sites were observed and we were able to determine ACR adduction levels at discrete sites within a protein. ADP/ATP-translocase 1 (ANT1) is a well-described target of oxidative modification reactions [36, 40, 41]. ANT1 has four cysteine residues, and in this study we were able to assess ACR adduction levels at Cys-159 and Cys-256. ANT1 undergoes complex conformational transitions during transport of adenine nucleotides through the inner mitochondrial membrane [38]. Earlier studies in which thiol reagents were used as conformational probes indicated that that Cys-159 was highly reactive and accessible to a diverse set of thiol probes in contrast to Cys-256 [42]. Indeed, ACR adduction at Cys-159 was found to be higher than on Cys-256. We and others have previously identified malate dehydrogenase as a protein which is susceptible to modifications by 2-enals [25, 36, 43, 44]. Malate dehydrogenase is a TCA cycle protein and has six cysteine residues. In this study, ACR adduction

was consistently observed at Cys-93 and Cys-212. As part of our earlier study, we have extracted B-Factors, an index of protein dynamics, and surface accessible area (SAA) values for the cysteine residues from the published X-ray structure of malate dehydrogenase (pdb 1MLD) [36]. The higher adduction levels observed for Cys-212 are consistent with the higher B-Factor and SAA value observed for Cys-212 (B-Factor 33.71, SAA 45.95) compared with Cys-93 (B-Factor 26.27, SAA 20.55).

3.6 Quantification of myocardial protein–ACR adducts in an animal model of in vivo oxidative stress

Next, we used our differential labeling strategy in combination with LC-MS/MS SRM for determining relative levels of protein–ACR adducts in cardiac mitochondria from 3-month-old rats that were administered CCl_4 intraperitoneally, an accepted in vivo model of acute oxidative stress [45]. Urine samples collected from the same rats in this experiment had elevated levels of metabolites of 4-hydroxy-2-nonenal and 4-oxo-2-nonenal compared to control animals, indicating that these urinary metabolites are indeed products of CCl_4-induced lipid peroxidation [46]. Metabolites of ACR were not analyzed for in this study. The relative levels of peptide ACR-adducts and peptide thiols were determined in the control and the CCl_4-exposed animal group. Figure 4 shows that the mean ratios of ACR-modified peptide to the unmodified peptide thiol were higher in the CCl_4-treated animals than those in control rats for all seven peptides **a**–**g** listed in Table 2. CCl_4-treatment resulted in significant ratio differences for peptides **b**, **c**, **d**, **f** and **g** with p-values < 0.05. There was insufficient statistical difference for the other peptides (**a** and **e**), but, the trend was conserved that CCl_4-exposure resulted in increased ACR adduction levels in relation to the respective peptide thiol pool. These results indicate that ACR-modified proteins may have value as mitochondrial markers of oxidative stress.

ACR is formed via multiple routes, e.g. from metabolism of allyl compounds, lipid peroxidation of polyunsaturated fatty acids, and from oxidative metabolism of polyamines by amine oxidases. ACR is known to be the most reactive of the α,β-unsaturated aldehydes. Although the ARP labeling strategy is generally applicable to aldehydic protein modification, only ARP-labeled ACR adducts were reproducibly detected and quantified in this study. A possible reason for the selective detection of protein–ACR adducts is that they, unlike lipid-derived 4-hydroxy-2-enals, cannot form cyclic hemiacetals that would interfere with ARP labeling. Michael-type protein adducts of 4-hydroxy-2-enals, e.g. HNE, may partially escape ARP labeling due to their formation of cyclic hemiacetals with reduced reactivity toward ARP [13]. Alternatively, the greater reactivity of ACR toward protein thiols compared with other alkenals may also contribute to the bias toward cysteine-ACR adducts in the current data set

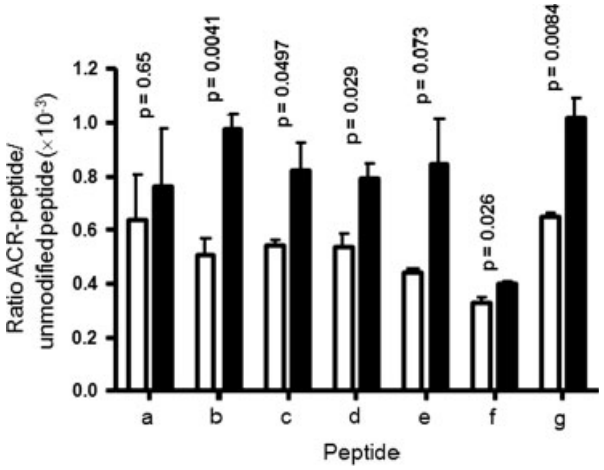

Figure 4. Ratios of ACR-modified peptide to the respective unmodified thiol-peptide for control rats ($n = 3$, white bars) and CCl_4-treated rats ($n = 3$, black bars): (A), EFNGLGD**C**LTK (Cys-159) and (B), GADIMYTGTVD**C**WR (Cys-256) from ADP/ATP translocase 1 (ADT1_RAT, Q05962); (C), N**C**AQFVTGSQAR (Cys-100) from ATP synthase d chain (ATP5H_RAT, P31399); (D), GGDVSV**C**EWYR (Cys-54), from cytochrome c oxidase subunit VIb isoform 1 (CX6B1_Mouse, P56391; gene bank accession number for the corresponding rat protein: EDM07730); (E), LVEG**C**LVGGR (Cys-100) from NADH dehydrogenase [ubiquinone] flavoprotein 1 (NDUV1_MOUSE, Q91YT0; gene bank accession number for the corresponding rat protein: AAH83709); (F), G**C**DVVVIPAGVPR (Cys-93) and (G), TIIPLISQ**C**TPK (Cys-212) from malate dehydrogenase (MDHM_RAT, P04635). All results are presented as the mean ± SEM.

[5, 13]. The reported data only represent a subset of possible ACR modifications, namely Michael-type adducts of ACR to cysteine residues. For this reason, a limitation of the reported method is that it fails to quantify other possible ACR modifications, such as Schiff's base-type modification, FDP-lysine modification and possible cross-links [47]. For comparison, Judge et al. reported 0.26 nmol protein carbonyl/mg protein for SSM sample using an immunoassay [48].

4 Concluding remarks

Overall, we have developed an analytical strategy that enables the quantification of Michael-type protein adducts of ACR in complex biological mixtures. Our approach combines the identification and relative quantification of ACR-modified proteins by nanoLC MS/MS SRM analysis. In addition, the method provides information on specific amino acids that are modified by ACR, their location and their extent of modification in a protein. We have shown that the ratios of ACR adduction level to thiol level at a distinct site have value as a marker of oxidative stress. This strategy is not limited to ACR adducts of proteins but could also be applied to determine levels of adduction by other 2-enals. The method has made inroads into assessment of the in vivo ACR status as a function of oxidant stress in

health and disease. The analytical strategy should be equally applicable to heat-processed foods in which thermally produced ACR forms adducts with proteins.

The authors thank Dr. Cristobal Miranda for animal husbandry. This work was supported by NIH grants R01 AG025372 (Maier), S10 RR022589 and R01 HL081721 (Stevens). The OSU EHSC mass spectrometry facility and core is supported in part by the Environmental Health Sciences Center (P30 ES00210).

The authors have declared no conflict of interest.

5 References

[1] Faroon, O., Roney, N., Taylor, J., Ashizawa, A. et al., Acrolein health effects. *Toxicol. Ind. Health* 2008, *24*, 447–490.

[2] Stevens, J. F., Maier, C. S., Acrolein: sources, metabolism, and biomolecular interactions relevant to human health and disease. *Mol. Nutr. Food Res.* 2008, *52*, 7–25.

[3] Minko, I. G., Kozekov, I. D., Harris, T. M., Rizzo, C. J. et al., Chemistry and biology of DNA containing 1,N(2)-deoxyguanosine adducts of the alpha,beta-unsaturated aldehydes acrolein, crotonaldehyde, and 4-hydroxynonenal. *Chem. Res. Toxicol.* 2009, *22*, 759–778.

[4] Uchida, K., Current status of acrolein as a lipid peroxidation product. *Trends Cardiovasc. Med.* 1999, *9*, 109–113.

[5] LoPachin, R. M., Gavin, T., Petersen, D. R., Barber, D. S., Molecular mechanisms of 4-hydroxy-2-nonenal and acrolein toxicity: nucleophilic targets and adduct formation. *Chem. Res. Toxicol.* 2009, *22*, 1499–1508.

[6] Custovic, Z., Zarkovic, K., Cindric, M., Cipak, A. et al., Lipid peroxidation product acrolein as a predictive biomarker of prostate carcinoma relapse after radical surgery. *Free Radic. Res.* 2010, *44*, 497–504.

[7] Srivastava, S., Sithu, S. D., Vladykovskaya, E., Haberzettl, P. et al., Oral exposure to acrolein exacerbates atherosclerosis in apoE-null mice. *Atherosclerosis* 2011, *215*, 301–308.

[8] Hamann, K., Shi, R., Acrolein scavenging: a potential novel mechanism of attenuating oxidative stress following spinal cord injury. *J. Neurochem.* 2009, *111*, 1348–1356.

[9] Bradley, M. A., Markesbery, W. R., Lovell, M. A., Increased levels of 4-hydroxynonenal and acrolein in the brain in preclinical Alzheimer disease. *Free Radic. Biol. Med.* 2010, *48*, 1570–1576.

[10] Zarkovic, K., Uchida, K., Kolenc, D., Hlupic, L., Zarkovic, N., Tissue distribution of lipid peroxidation product acrolein in human colon carcinogenesis. *Free Radic. Res.* 2006, *40*, 543–552.

[11] Shi, Y., Sun, W., McBride, J. J., Cheng, J.-X., Shi, R., Acrolein induces myelin damage in mammalian spinal cord. *J. Neurochem.* 2011, *117*, 554–564.

[12] Luo, J., Hill, B. G., Gu, Y., Cai, J. et al., Mechanisms of acrolein-induced myocardial dysfunction: implications for environmental and endogenous aldehyde exposure. *Am. J. Physiol. Heart Circ. Physiol.* 2007, *293*, H3673–H3684.

[13] Sayre, L. M., Lin, D., Yuan, Q., Zhu, X., Tang, X., Protein adducts generated from products of lipid oxidation: focus on HNE and one. *Drug Metab. Rev.* 2006, *38*, 651–675.

[14] Stadtman, E. R., Protein oxidation in aging and age-related diseases. *Ann. NY Acad. Sci.* 2001, *928*, 22–38.

[15] Lund, M. N., Heinonen, M., Baron, C. P., Estévez, M., Protein oxidation in muscle foods: a review. *Mol. Nutr. Food Res.* 2011, *55*, 83–95.

[16] Levine, R. L., Garland, D., Oliver, C. N., Amici, A. et al., Determination of carbonyl content in oxidatively modified proteins. *Methods Enzymol.* 1990, *186*, 464–478.

[17] Korolainen, M. A., Goldsteins, G., Alafuzoff, I., Koistinaho, J., Pirttila, T., Proteomic analysis of protein oxidation in Alzheimer's disease brain. *Electrophoresis* 2002, *23*, 3428–3433.

[18] Reinheckel, T., Korn, S., Mohring, S., Augustin, W. et al., Adaptation of protein carbonyl detection to the requirements of proteome analysis demonstrated for hypoxia/reoxygenation in isolated rat liver mitochondria. *Arch. Biochem. Biophys.* 2000, *376*, 59–65.

[19] Ichihashi, K., Osawa, T., Toyokuni, S., Uchida, K., Endogenous formation of protein adducts with carcinogenic aldehydes. *J. Biol. Chem.* 2001, *276*, 23903–23913.

[20] Roeser, J., Bischoff, R., Bruins, A., Permentier, H., Oxidative protein labeling in mass-spectrometry-based proteomics. *Anal. Bioanal. Chem.* 2010, *397*, 3441–3455.

[21] Chavez, J., Wu, J., Han, B., Chung, W. G., Maier, C. S., New role for an old probe: affinity labeling of oxylipid protein conjugates by N′-aminooxymethylcarbonylhydrazino d-biotin. *Anal. Chem.* 2006, *78*, 6847–6854.

[22] Barnes, S., Shonsey, E. M., Eliuk, S. M., Stella, D. et al., High-resolution mass spectrometry analysis of protein oxidations and resultant loss of function. *Biochem. Soc. Trans.* 2008, *36*, 1037–1044.

[23] Roede, J. R., Carbone, D. L., Doorn, J. A., Kirichenko, O. V. et al., In vitro and in silico characterization of peroxiredoxin 6 modified by 4-hydroxynonenal and 4-oxononenal. *Chem. Res. Toxicol.* 2008, *21*, 2289–2299.

[24] Roe, M. R., Xie, H., Bandhakavi, S., Griffin, T. J., Proteomic mapping of 4-hydroxynonenal protein modification sites by solid-phase hydrazide chemistry and mass spectrometry. *Anal. Chem.* 2007, *79*, 3747–3756.

[25] Han, B., Stevens, J. F., Maier, C. S., Design, synthesis, and application of a hydrazide-functionalized isotope-coded affinity tag for the quantification of oxylipid-protein conjugates. *Anal. Chem.* 2007, *79*, 3342–3354.

[26] Madian, A. G., Regnier, F. E., Proteomic identification of carbonylated proteins and their oxidation sites. *J. Proteome Res.* 2010, *9*, 3766–3780.

[27] Madian, A. G., Regnier, F. E., Profiling carbonylated proteins in human plasma. *J. Proteome Res.* 2010, *9*, 1330–1343.

[28] Codreanu, S. G., Zhang, B., Sobecki, S. M., Billheimer, D. D., Liebler, D. C., Global Analysis of protein damage by the

lipid electrophile 4-hydroxy-2-nonenal. *Mol. Cell. Proteomics* 2009, *8*, 670–680.

[29] Maier, C. S., Chavez, J., Wang, J., Wu, J. et al., *Methods Enzymology*, Academic Press, New York pp. 305–330.

[30] Carini, M., Aldini, G., Facino, R. M., Mass spectrometry for detection of 4-hydroxy-trans-2-nonenal (HNE) adducts with peptides and proteins. *Mass Spectrom Rev.* 2004, *23*, 281–305.

[31] Orioli, M., Aldini, G., Benfatto, M. C., Maffei Facino, R., Carini, M., HNE Michael adducts to histidine and histidine-containing peptides as biomarkers of lipid-derived carbonyl stress in urines:LC MS/MS profiling in Zucker Obese rats. *Anal. Chem.* 2007, *79*, 9174–9184.

[32] Held, J. M., Danielson, S. R., Behring, J. B., Atsriku, C. et al., Targeted quantitation of site-specific cysteine oxidation in endogenous proteins using a differential alkylation and multiple reaction monitoring mass spectrometry approach. *Mol. Cell. Proteomics* 2010, *9*, 1400–1410.

[33] Chung, H., Hong, D. P., Jung, J. Y., Kim, H. J. et al., Comprehensive analysis of differential gene expression profiles on carbon tetrachloride-induced rat liver injury and regeneration. *Toxicol. Appl. Pharmacol.* 2005, *206*, 27–42.

[34] Srinivasan, R., Chandrasekar, M. J., Nanjan, M. J., Suresh, B., Antioxidant activity of *Caesalpinia digyna* root. *J. Ethnopharmacol.* 2007, *113*, 284–291.

[35] Palmer, J. W., Tandler, B., Hoppel, C. L., Biochemical properties of subsarcolemmal and interfibrillar mitochondria isolated from rat cardiac muscle. *J. Biol. Chem.* 1977, *252*, 8731–8739.

[36] Chavez, J. D., Wu, J., Bisson, W., Maier, C. S., Site-specific proteomic analysis of lipoxidation adducts in cardiac mitochondria reveals chemical diversity of 2-alkenal adduction. *J. Proteomics* 2011, DOI: 10.1016/jprot.2011.03.031.

[37] Chavez, J., Chung, W.-G., Miranda, C. L., Singhal, M. et al., Site-specific protein adducts of 4-hydroxy-2(E)-nonenal in human thp-1 monocytic cells: protein carbonylation is diminished by ascorbic acid. *Chem. Res. Toxicol.* 2009, *23*, 37–47.

[38] Klingenberg, M., The ADP and ATP transport in mitochondria and its carrier. *Biochim. Biophys. Acta* 2008, *1778*, 1978–2021.

[39] Gibson, B. W., The human mitochondrial proteome: oxidative stress, protein modifications and oxidative phosphorylation. *Int. J. Biochem. Cell Biol.* 2005, *37*, 927–934.

[40] Chung, W.-G., Miranda, C. L., Maier, C. S., Detection of carbonyl-modified proteins in interfibrillar rat mitochondria using N′-aminooxymethylcarbonylhydrazino-D-biotin as an aldehyde/keto-reactive probe in combination with Western blot analysis and tandem mass spectrometry. *Electrophoresis* 2008, *29*, 1317–1324.

[41] Yan, L. J., Sohal, R. S., Prevention of flight activity prolongs the life span of the housefly, *Musca domestica*, and attenuates the age-associated oxidative damage to specific mitochondrial proteins. *Free Radic. Biol. Med.* 2000, *29*, 1143–1150.

[42] Majima, E., Koike, H., Hong, Y. M., Shinohara, Y., Terada, H., Characterization of cysteine residues of mitochondrial ADP/ATP carrier with the SH-reagents eosin 5-maleimide and N-ethylmaleimide. *J. Biol. Chem.* 1993, *268*, 22181–22187.

[43] Sultana, R., Newman, S. F., Abdul, H. M., Cai, J. et al., Protective effect of D609 against amyloid-beta1-42-induced oxidative modification of neuronal proteins: redox proteomics study. *J. Neurosci. Res.* 2006, *84*, 409–417.

[44] Reed, T. T., Pierce, W. M., Markesbery, W. R., Butterfield, D. A., Proteomic identification of HNE-bound proteins in early Alzheimer disease: insights into the role of lipid peroxidation in the progression of AD. *Brain Res.* 2009, *1274*, 66–76.

[45] Halliwell, B., Gutteridge, T., *Free Radic. Biol. Med.*, Oxford University Press, London 2007.

[46] Kuiper, H. C., Miranda, C. L., Sowell, J. D., Stevens, J. F., Mercapturic acid conjugates of 4-hydroxy-2-nonenal and 4-oxo-2-nonenal metabolites are in vivo markers of oxidative stress. *J. Biol. Chem.* 2008, *283*, 17131–17138.

[47] Cai, J., Bhatnagar, A., Pierce, W. M., Jr., Protein modification by acrolein: formation and stability of cysteine adducts. *Chem. Res. Toxicol.* 2009, *22*, 708–716.

[48] Judge, S., Jang, Y. M., Smith, A., Hagen, T., Leeuwenburgh, C., Age-associated increases in oxidative stress and antioxidant enzyme activities in cardiac interfibrillar mitochondria: implications for the mitochondrial theory of aging. *FASEB J.* 2005, *19*, 419–421.

